IEEE Access
Multidisciplinary | Rapid Review | Open Access Journal

Received May 15, 2020, accepted May 30, 2020, date of publication June 2, 2020, date of current version June 17, 2020.

Digital Object Identifier 10.1109/ACCESS.2020.2999519

A Linear Integer Programming Model for Fault Diagnosis in Active Distribution Systems With Bi-Directional Fault Monitoring Devices Installed

CHONGYU WANG[1], (Graduate Student Member, IEEE), KAIYUAN PANG[1], (Graduate Student Member, IEEE), YAN XU[2], FUSHUAN WEN[3], (Senior Member, IEEE), IVO PALU[3], (Member, IEEE), AND CHANGSEN FENG[4], (Member, IEEE)

[1]School of Electrical Engineering, Zhejiang University, Hangzhou 310027, China
[2]School of Electrical and Information Engineering, Changsha University of Science and Technology, Changsha 410114, China
[3]Department of Electrical Power Engineering and Mechatronics, Tallinn University of Technology, 19086 Tallinn, Estonia
[4]College of Information Engineering, Zhejiang University of Technology, Hangzhou 310000, China

Corresponding author: Fushuan Wen (fushuan.wen@taltech.ee)

This work was jointly supported in part by the National Key Research and Development Program of China under Grant 2017YFB0902900, in part by the National Natural Science Foundation of China under Grant 51807009 and Grant 71931003, and in part by the Special Funding for the Construction of Innovative Hunan Province under Grant 2019RS1045.

ABSTRACT With the extensive installation of intelligent electronic devices with bi-directional fault monitoring capabilities, richer fault direction information can be collected and utilized to achieve an accurate fault diagnosis. In this paper, we consider the fault diagnosis problem in active distribution systems with distributed generators connected, such as rotating electrical machine power sources and centralized inverter interfaced renewable energy resources. The fault diagnosis problem is modeled as a linear integer programming problem with an objective to minimize the numbers of fault zones and false alarms. A novel functional form is derived to capture the expected alarms sent by bi-directional fault monitoring devices to be compared with the actual alarms received by the dispatch center. Uncertainties in both the monitoring and communication stages are considered in the model by formulating the numbers of false alarms in the objective function. Three types of suspected false alarms can be detected: "missing alarms", "distorted alarms", and "reverse alarms". By solving the developed optimization model for fault diagnosis, false alarms and suspected fault zones can be found. Case studies in a modified IEEE 33-bus system and a 55-bus system in Guangzhou, China are carried out in several different scenarios with multiple faults to demonstrate the performance of the proposed model. Numerical tests show that the proposed approach is superior in computational time such that it can be used for real-time fault diagnosis in active distribution systems.

INDEX TERMS Active distribution system, bi-directional fault monitoring devices, fault diagnosis, linear integer programming.

I. INTRODUCTION

With the rapid construction of distribution systems worldwide, especially urban distribution systems, efficient system troubleshooting has become increasingly important. Fault location, isolation and service restoration (FLISR) are the three main steps of self-healing for power systems [1]. The fault location, as the first of these three steps, is influential to the effectiveness and efficiency of the entire FLISR process. As distributed generators (DGs) are extensively connected to distribution systems, conventional power distribution systems are being reshaped into active distribution networks [2]. This development increases the complexity of fault location issues.

Due to the acquisition and uploading of more sensor information, the automation of modern power systems is constantly being improved, which enables accurate fault diagnosis under information redundancy. However, power distribution systems have in general fewer sensors (called monitoring devices) than power transmission systems. As more attention is being paid to the monitoring of power distribution systems, a large number of intelligent electronic devices (IEDs) have been adopted. Nowadays, IEDs have been used to communicate with gateways of supervisory control and data acquisition (SCADA) systems in accordance

The associate editor coordinating the review of this manuscript and approving it for publication was Vigna K. Ramachandaramurthy.

with specified protocols [3], by providing data to be captured by dispatching centers. In recent years, SCADA systems that collect and process data generated by IEDs have been extensively installed in power distribution systems.

Fault indicators (FIs), as the representatives of IEDs, are extensively installed in power distribution systems due to reliable performance and low cost [4], [5]. Unlike most impedance-based fault location methods, the approach proposed in [6] does not assume that all feeder sections have the same impedance characteristics, and uses the indication information of FIs to improve the accuracy of fault location. In [7], a matrix-based approach is used for automated fault diagnosis, which reveals the relationship between possible fault segments and fault currents detected by FIs. In [8], a downstream marking algorithm utilizing status information generated by FIs is proposed, which is more accurate than a conventional upstream marking one. Reference [9] determines a final fault area based on evidence information obtained from FIs, distribution transformers, and trouble calls, using an improved Dempster-Shafer theory. Unfortunately, the methods proposed in [6]–[9] have not specifically addressed fault diagnosis in active power distribution systems, where power flow changes can be bi-directional, making these methods unadaptable.

A distribution-level phasor measurement unit (D-PMU) [10], also called a micro phasor measurement unit (μ PMU) [11] for its small volume, is one type of monitoring device installed in a power distribution system capable of sampling voltage and current data with a high frequency, which makes online fault analysis available [12]. In [13], fault location is found by iteratively checking voltage and current data of each segment recorded by D-PMUs such that this method can be implemented in distribution systems with DGs connected. In [12], a method for real-time fault monitoring of active distribution systems is proposed by calculating state estimation of parallel synchronized phasors. Since vector monitoring data can be acquired by D-PMUs, they can be implemented in active distribution systems to indicate fault areas.

As pointed out in [8] and [14], some unique bi-directional FIs can indicate not only faults in a single preset direction, but also faults in both upstream and downstream directions. In terms of indicating faults in bi-directions, D-PMUs can function similarly as bi-directional FIs. Additionally, feeder termination units (FTUs) can also provide indications of three fault monitoring states, which have been explained in [15] and [16]. In [15], an analytic fault diagnosis method is established, which can find suspected fault sections correctly even in some scenarios where the measurements of some FTUs are unreliable. In [16], a linear integer model based on states sent by FTUs is proposed to provide the globally optimal fault segment location of an active distribution network. This method, however, can only find a single fault in [16], instead of multiple faults.

As more and more remote residential areas and industrial factories need to be powered, the multi-branch topology of modern urban distribution systems has become increasingly complicated, rendering the corresponding fault location [17], [18] or fault zones estimation [19]–[21] issues research hotspots. The method proposed in earlier literature is based on the analysis of physical circuits, such as the direct circuit analysis method proposed in [17] and the impedance-based calculation method proposed in [20]. And the methods proposed in some recent pieces of literature are based on the fusion of multiple methods, such as the multi-sensor fusion method proposed in [18] and the method based on the natural frequency components of fault voltages proposed by [21].

Moreover, the urgent need for power supply may prioritize the construction of physical systems above reliable communication systems, which leads to delays in the collection and analysis of monitoring data related to faults. Reference [22] pointed out that sensor faults may lead to a decline in diagnostic performance, and a data-driven Bayesian network-based three-phase inverter fault diagnosis method is proposed to solve this matter. In [23], dynamic Bayesian networks are used to solve the degradation problem of structural systems caused by the coupling of multiple factors. Aiming at the problem that the performance of electronic products will decrease with time, the method proposed in [24] uses dynamic Bayesian networks to characterize the dynamic degradation process of electronic products. Additionally, as pointed out in [18] and [17], without reliable communication systems, the alarms sent by IEDs may not be reliable at all. The malfunction of any measuring devices and/or the block of communication channels under extreme conditions may further contribute to missing or distorted alarms.

This paper will address two important tasks in fault diagnosis problems: the estimation of fault zones and the identification of false alarms. A linear integer programming model utilizing alarms sent by bi-directional fault monitoring devices is proposed in this paper to address fault diagnosis issues in active power distribution systems. The major contributions of this paper are summarized as follows:

1) The concepts of generalized upstream and downstream power supply paths are given for bi-directional fault monitoring devices (such as D-PMUs, FTUs, bi-directional FIs) installed in active power distribution systems. Then, a novel expected alarm function for bi-directional fault monitoring devices is proposed, which can be used in scenarios with multiple faults. By changing the input values of the corresponding variables, the expected alarm function can be easily adapted to model changes in the topology of the distribution system and the connection state of each DG.

2) To address the problems of fault diagnosis, the identification of fault zones and false alarms can be obtained together by solving the proposed model. In particular, the false alarms sent by the bi-directional fault monitoring device are classified into three types: "reverse alarms", "distorted alarms", and "missing alarms", whose evaluation states are given different weights in the objective function.

3) The fault diagnosis problem is modeled as a linear integer programming problem, which means that the relevant objective function and constraints can be equivalently

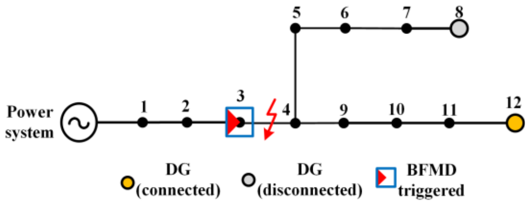

FIGURE 1. A sample distribution system with a BFMD installed.

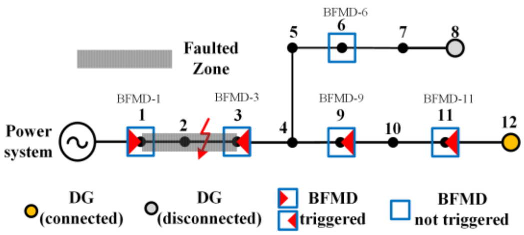

FIGURE 2. The integration of multiple BFMDs in a sample distribution system with a single fault.

represented in a linear form. Therefore, the global optimal fault diagnosis hypothesis can be obtained using existing rigorous approaches, instead of heuristic algorithms that can only find local optima.

II. FUNCTIONS OF BI-DIRECTIONAL FAULT MONITORING DEVICES IN ACTIVE POWER DISTRIBUTION SYSTEMS

A. BI-DIRECTIONAL FAULT MONITORING DEVICES

In distribution systems with DGs (e.g., diesel engines, gas engines and centralized renewable energy resources), fault related alarms generated by IEDs with bi-directional overcurrent monitoring capabilities can be classified into three types: 1) fault(s) are detected upstream; 2) fault(s) are detected downstream; and 3) no fault detected.

To facilitate the presentation, the IEDs which are capable of generating these three monitored fault states of alarms, including D-PMUs, FTUs and bi-directional FIs, are collectively referred to as bi-directional fault monitoring devices (BFMDs) hereinafter. In order to clarify the function of BFMDs, a sample power distribution system with a single fault is shown in Fig. 1.

The direction of the overcurrent flowing through the BFMD is consistent with the red triangle in Fig. 1. When the distribution feeder is operating well, the BFMD is triggered only when the monitored current value or its rising rate exceeds the threshold. As can be seen in Fig. 1, when a permanent ground fault occurs on the line, the BFMD is triggered by an overcurrent. Obviously, when the load on the feeder is powered by a single-sided supply, the BFMD will be triggered by a fault that occurs downstream of its installation location. Since only one BFMD is not sufficient in indicating the fault location, the integration of multiple BFMDs is needed, which is presented in Fig. 2.

As shown in Fig. 2, five BFMDs are installed, which are located near buses 1, 3, 6, 9, and 11, respectively. Since BFMD-1 is triggered with the downstream direction, the fault may be located in the downstream of it. Suppose that BFMD-3, BFMD-9 and BFMD-11 are also triggered and indicate the fault location in the upstream of them. The fault can be determined in the shaded zone by the integration of these four triggered BFMDs. It can be seen from this simple example that the fault state of BFMDs being triggered or not corresponds uniquely to the fault location.

An obvious challenge is how to maximize the accuracy of fault diagnosis if false alarms may be received by the dispatching center. This prompts us to develop a fault diagnosis model that can accommodate false alarms.

III. GENERALIZED UPSTREAM AND DOWNSTREAM POWER SUPPLY PATHS OF BFMDs IN AN ACTIVE POWER DISTRIBUTION SYSTEM

Prior to introducing the proposed optimization model for fault diagnosis, it is necessary to clarify the definition of the forward and backward directions and the generalized upstream and downstream paths of BFMDs installed in an active distribution system.

A. FORWARD AND BACKWARD DIRECTIONS OF BFMD

When the power distribution system is only powered by the grid side (i.e., without connecting to any DGs), the power direction flowing through a BFMD is called the forward direction of the BFMD when there is no fault, and the opposite direction is called the backward direction of this BFMD.

B. GENERALIZED UPSTREAM AND DOWNSTREAM POWER SUPPLY PATH

The paths from where a BFMD is installed to all power supply nodes that can provide a positive short circuit current to this BFMD is referred to as the generalized upstream paths of this BFMD in this work. Similarly, the paths from the installation location of a BFMD to all power supply nodes that can provide a negative short circuit current to this BFMD is referred to as the generalized downstream paths of this BFMD. Taking BFMD-3 in Fig. 2 as an example, the highlighted faulted zone (around nodes-1,2,3) can be referred to as its upstream power supply path, while the zones between nodes-3, 4, 9, 10, 11, and 12 can be referred to as BFMD-3's downstream power supply path. Furthermore, if the DG located at node-8 in Fig. 2 is connected to the distribution system, the generalized downstream paths of BFMD-3 consist of the zones between nodes 3, 4, 9, 10, 11,12 and the zones between nodes 4, 5, 6, 7, 8 together.

IV. LINEAR INTEGER PROGRAMMING MODEL FOR FAULT DIAGNOSIS

The proposed fault diagnosis model consists of an objective function and BFMD related constraints. The nonlinear formulation will be introduced first, followed by its linearization form.

A. THE OBJECTIVE FUNCTION AND RELATED CONSTRAINTS

A comprehensive objective function is introduced to address the two basic functions of fault diagnosis: fault zones estimation and the identification of false alarms. Therefore, the objective function $E(\boldsymbol{L})$ consists of the sum of the number of suspected fault zones N_f and the number of false alarms WR_{BFMD}, as shown in(1); both numbers are to be minimized:

$$E(\boldsymbol{L}) = N_f + \boldsymbol{WR}_{\mathrm{BFMD}} \tag{1}$$

where $\boldsymbol{L} = [l_1, l_2, \ldots, l_{NL}]$ is the fault state vector of all zones separated by BFMDs on the feeder; each element in $\boldsymbol{L}$ is a binary variable, which takes the value of 1 when a fault occurs on the corresponding zone and 0 when there is no fault, and NL is the number of zones separated by BFMDs. The two terms in the objective function are detailed in (2) and (3).

$$N_f = \sum_{m=1}^{NL} l_m \tag{2}$$

Suspected false alarms are classified as the missing, distorted or reverse alarms, whose meanings are described as follows:

1) A missing alarm: an alarm has been sent by a BFMD but has not been received by the dispatch center.

2) A distorted alarm: an alarm received by the dispatch center should not have been sent by a BFMD.

3) A reverse alarm: an alarm received by the dispatch center has the indicated fault direction opposite to the expected one.

$$WR_{\mathrm{BFMD}} = \omega_{\mathrm{BFMD}} \sum_i M_{\mathrm{BFMD},i} + \beta_{\mathrm{BFMD}} \sum_i D_{\mathrm{BFMD},i} + \gamma_{\mathrm{BFMD}} \sum_i R_{\mathrm{BFMD},i} \quad \forall i \in \Psi \tag{3}$$

where WR_{BFMD} is the penalty function of false alarms sent by BFMDs; Ψ is the index set of the nodes where BFMDs are installed; $M_{\mathrm{BFMD},i}$ is a binary variable whose value is 1 if the alarm sent by BFMD-i (a shorthand for the BFMD at node i) is missing. $D_{\mathrm{BFMD},i}$ is a binary variable whose value is 1 if the alarm sent by BFMD-i is distorted; $R_{\mathrm{BFMD},i}$ is defined similarly for a reverse alarm send by BFMD-i. Parameters ω_{BFMD}, β_{BFMD} and γ_{BFMD} are penalty coefficients of these three different types of false alarms.

If an alarm triggered by a BFMD is received by the dispatch center, the actual alarm function of this BFMD is positive and shall take the value of 1; otherwise the outcome is negative and will take the value of 0. Nevertheless, the expected alarms sent by BFMDs subject to an actual fault scenario may not be consistent with the corresponding alarms actually received. To identify false alarms, it is necessary to compare the expected alarms that BFMDs should send with the actual alarms received by the dispatching center. Therefore, the "expected alarm function" of a BFMD needs to be defined.

B. BFMDs RELATED CONSTRAINTS

1) THE EXPECTED ALARM FUNCTIONS SENT BY BFMDs WITH A SINGLE FAULT

The expected alarms sent by bi-directional FIs have been studied in [16], using the notion of a "switch function". In terms of the variables used in this paper, this function is shown in (4).

$$G_i^* = (\boldsymbol{P}_{down,i})^{\mathrm{T}}\boldsymbol{L} - k_{DG,i}(\boldsymbol{P}_{up,i})^{\mathrm{T}}\boldsymbol{L} \quad \forall i \in \Psi \tag{4}$$

where G_i^* is the expected alarms sent by bi-directional FIs; $k_{DG,i}$ is a binary variable indicating the connection state of DGs on the generalized downstream path of FI-i. When $k_{DG,i} = 1$ (or 0), it means that at least one DG is (or not) connected; $\boldsymbol{P}_{down,i}$ and $\boldsymbol{P}_{up,i}$ are the binary vector of generalized downstream and upstream with the BFMD installed at node-i, respectively. Specifically, in IV-B2 if the segment is on the generalized downstream path or the generalized upstream path of FI-i described in Section III-B, the value of the corresponding element in $\boldsymbol{P}_{down,i}$ or $\boldsymbol{P}_{up,i}$ is taken as 1, otherwise it is taken as 0.

Note that although the expected alarm function in IV-B2 is concise, it is only applicable to scenarios with a single fault. Next we shall extend the switch function in IV-B2 to a more general expected alarm function applicable to situations with multiple faults.

2) THE EXPECTED ALARM FUNCTIONS OF BFMDs WITH MULTIPLE FAULTS

The expected alarm sent by BFMD-i applicable to the scenarios with multiple faults can be calculated by (5)-(7) below.

$$F_i^* = F_{forw,i} - F_{bacw,i} \quad \forall i \in \Psi \tag{5}$$

$$F'_{forw,i} = (1 - \boldsymbol{W}_{grid,i}^{\mathrm{T}}\boldsymbol{L}) + \sum_n k_{DG,n}(1 - \boldsymbol{W}_{up,i,n}^{\mathrm{T}}\boldsymbol{L}) \quad \forall i \in \Psi,\ n \in \Upsilon_{up,i} \tag{6}$$

$$F'_{bacw,i} = \sum_n k_{DG,n}(1 - \boldsymbol{W}_{down,i,n}^{\mathrm{T}}\boldsymbol{L}) \quad \forall i \in \Psi,\ n \in \Upsilon_{down,i} \tag{7}$$

In (5), given BFMD-i F_i^* represents the BFMD's expected alarm; $F_{forw,i}$ is a binary variable indicating whether the power supplies (including DGs) located in the BFMD's generalized upstream direction (defined in Section III-B) can provide overcurrent to the forward direction (defined in Section III-A) of BFMD-i. Similarly, $F_{bacw,i} = 1/0$ represents whether the power supplies (including DGs) located in the BFMD's generalized downstream direction can provide overcurrent to the backward direction of the BFMD.

In (5)-(6), $\Upsilon_{up,i}$ and $\Upsilon_{up,i}$ are the index sets of the nodes connected with the DG(s) in the generalized upstream and the generalized downstream directions of BFMD-i, respectively; $F'_{forw,i}$ (or $F'_{bacw,i}$) represents a binary variable indicating whether the forward (or backward) overcurrent through BFMD-i exists; $\boldsymbol{W}_{grid,i}$ is a vector whose size is the number of zones to be diagnosed, where each binary element, say the k-th, indicates whether the k-th line zone is on the path

TABLE 1. Meaningful/optional values of F_i^* and their meanings.

Meanings of the expected alarm	Values of F_i^*
No overcurrent was detected by BFMD-i	0
A forward* overcurrent was detected by BFMD-i	+1
A backward* overcurrent was detected by BFMD-i	-1

*The forward and backward directions of a BFMD are defined in section III-A.

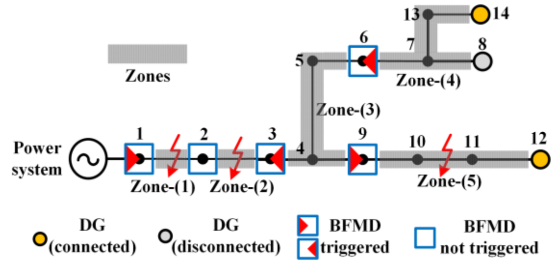

FIGURE 3. A sample distribution system with DGs-12,14 connected.

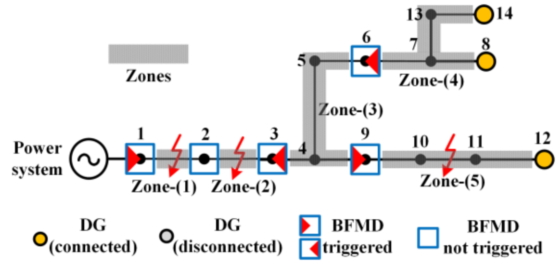

FIGURE 4. A sample distribution system with DGs-8,12,14 connected.

from the grid side (node-1, generally) to node-i; $\boldsymbol{W}_{up,i,n}$ and $\boldsymbol{W}_{down,i,n}$ are vectors of the same size as $\boldsymbol{W}_{grid,i}$, where each binary element, say the k-th, indicates whether the k-th line zone is on the path from node-i to node-n.

Regarding the intermittent characteristics of renewable energy resources, when the output power from a RER decreases to a certain threshold (determined by the specific fault monitoring devices) that cannot be detected by BFMDs installed at the upstream nodes, $k_{DG,i}$ can be set to 0. In addition, some centralized renewable energy resources are equipped with energy storage devices, such as battery energy storage systems, flywheel energy storage systems and compressed air energy storage systems, to smooth the output power profile and suppress the power output intermittence of a renewable energy generator.

Since BFMDs are capable of monitoring bi-directional overcurrent, the meaningful/optional values of F_i^* can be 0, +1 or −1, as presented in Table 1.

Note that as the value of $(\boldsymbol{W}_{grid,i})^{\mathrm{T}}\boldsymbol{L}$, $(\boldsymbol{W}_{up,i,n})^{\mathrm{T}}\boldsymbol{L}$ and $(\boldsymbol{W}_{down,i,n})^{\mathrm{T}}\boldsymbol{L}$ may be greater than 1 under the scenarios with multiple faults, the value of $F'_{forw,i}$ and $F'_{bacw,i}$ may be greater than 1 as well. To make (5) hold with the meaningful values of F_i^* in Table 1, $F_{forw,i}$ and $F_{bacw,i}$ need to be constrained by $F'_{forw,i}$ and $F'_{bacw,i}$ using linearization as described in (8)-(9).

$$\frac{F'_{forw,i}}{\mathrm{M}} \le F_{forw,i} \le F'_{forw,i} \quad \forall i \in \Psi,\ n_{DG} \in \Upsilon_{up,i} \tag{8}$$
$$\frac{F'_{bacw,i}}{\mathrm{M}} \le F_{bacw,i} \le F'_{bacw,i} \quad \forall i \in \Psi,\ n_{DG} \in \Upsilon_{down,i} \tag{9}$$

where M is a sufficiently large positive constant.

A detailed description of the expected alarm function shown in (5)-(9) will be illustrated by a sample distribution system with multiple faults in two scenarios, as presented in Fig. 3 and Fig. 4.

We will use BFMD-9 as an example to illustrate the idea of the proposed expected alarm functions. Although in this example the fault state vector $\boldsymbol{L}$ is a constant vector consistent with the fault scenario, it is a vector of variables in the actual diagnosis process.

In Fig. 3, since a fault occurred on the path between the grid side power supply (node 1) and BFMD-9, the first term $(1-\boldsymbol{W}_{grid,9}^{\mathrm{T}}\boldsymbol{L})$ in (6) is constrained to be 0. Note that DG-14 is also connected to the generalized upstream path of BFMD-9, and there is no fault on the path between them, so $k_{DG,14} = 1$ and the term $\boldsymbol{W}_{up,9,14}^{\mathrm{T}}\boldsymbol{L} = 0$ by (6). Therefore, $F_{forw,9} = F'_{forw,9} = 1$ can be obtained. Next, since DG-12 is connected in the generalized downstream path of BFMD-9, $k_{DG,12} = 1$ in (7) can be determined. However, as a fault zone is on the path between BFMD-9 and node-12, the term $\boldsymbol{W}_{down,9,12}^{\mathrm{T}}\boldsymbol{L} = 1$ is constrained to be 0. Therefore, $F_{bacw,9} = F'_{bacw,9} = 1$ can be obtained. To sum up, it can be determined that $F_9^* = 1$ in the scenario described in Fig. 3 by constraints (5)-(7).

Note in Fig. 4 the only difference from the analysis in Fig. 3 is that both DG-8 and DG-14 are connected to the generalized upstream path of BFMD-9, and no fault occurs on the path between these two DGs and BFMD-9. Thus, $k_{DG,8} = 1$, $\boldsymbol{W}_{up,9,8}^{\mathrm{T}}\boldsymbol{L} = 0$ and $k_{DG,14} = 1$, $\boldsymbol{W}_{up,9,14}^{\mathrm{T}}\boldsymbol{L} = 0$ can be determined; $F'_{forw,9} = 2$ can then be obtained. Using the linearization given in (8), $F_{forw,9} = 1$ and $F_9^* = 1$ are obtained within the required ranges.

As shown in Fig. 3 and Fig. 4, the two scenarios both have the same fault state set $\boldsymbol{L}$= [1,1,0,0,1]. As the connection states in these two figures are different, some values of the expected alarm functions sent by BFMDs are different, as presented in Table 2.

As shown in Table 2, in scenarios with multiple faults, the expected alarms of BFMD-3 and BFMD-6 in Fig. 4 are corrected by equation (9), and the expected alarm of BFMD-9 is constrained by equation (8). In these two different scenarios, all the expected alarms of BFMDs are calculated correctly by the formulas (5)-(9).

With the help of these two scenarios with multiple faults, the reason that the expected alarms of BFMDs calculated by IV-B2 may be incorrect is evident. In the scenario presented in Fig. 3 or Fig. 4, $G_9^* = -1$ can be obtained using (4), which means that the direction of the overcurrent flowing through BFMD-9 represented by the alarm is interpreted incorrectly. In addition, without the constraints such as (8) and (9), $G_6^* = -3$ is obtained by (4).

TABLE 2. Values of the expected alarm functions associated with each Bfmd in two scenarios.

Scenarios	BFMD	$F_{forw,i}'$	$F_{bacw,i}'$	$F_{forw,i}$	$F_{bacw,i}$	F_i^*
Fig. 3	BFMD-1	1	0	1	0	+1
	BFMD-2	0	0	0	0	0
	BFMD-3	0	1	0	1	-1
	BFMD-6	0	1	0	1	-1
	BFMD-9	1	0	1	0	+1
Fig. 4	BFMD-1	1	0	1	0	+1
	BFMD-2	0	0	0	0	0
	BFMD-3	0	2	0	1	-1
	BFMD-6	0	2	0	1	-1
	BFMD-9	2	0	1	0	+1

TABLE 3. Evaluation variables of false alarms.

F_i^*	F_i^{alarm}	Alarm's evaluation	Non-zero Values of Evaluation variables
0	0	Correct	/
+1	0	Missing	$M_{\mathrm{BFMD},i}$=1
0	+1	Distortion	$D_{\mathrm{BFMD},i}$ =1
+1	+1	Correct	/
-1	0	Missing	$M_{\mathrm{BFMD},i}$ =1
0	-1	Distortion	$D_{\mathrm{BFMD},i}$ =1
-1	-1	Correct	/
-1	+1	Reverse	$R_{\mathrm{BFMD},i}$ =1
+1	-1	Reverse	$R_{\mathrm{BFMD},i}$ =1

Where F_i^{alarm} represents the actual alarms received by the dispatching center.

3) MISSING/DISTORTED/REVERSE ALARMS AND THEIR RELATED CONSTRAINTS

The expected alarms of the bi-directional fault monitoring devices introduced previously are used to derive the expressions of false alarm states, including missing, distorted and reverse alarms. The relationships between these three types of alarms and the evaluation variables are illustrated in Table 3.

From the combination of all possible values of F_i^* and F_i^{alarm} presented in Table 3, the numerical logic of the evaluation variables, including M_{BFMD}, D_{BFMD} and R_{BFMD}, can be summarized as:

$$D_{\mathrm{BFMD},i} = \begin{cases} 1 & \text{when } F_i^* = 0 \text{ and } F_i^{alarm} \neq 0 \\ 0 & \text{otherwise} \end{cases} \quad \forall i \in \Psi \tag{10}$$

$$M_{\mathrm{BFMD},i} = \begin{cases} 1 & \text{when } F_i^{alarm} = 0 \text{ and } F_i^* \neq 0 \\ 0 & \text{otherwise} \end{cases} \quad \forall i \in \Psi \tag{11}$$

$$R_{\mathrm{BFMD},i} = \begin{cases} 1 & \text{when } F_i^* + F_i^{alarm} = 0 \\ & \quad \text{and } F_i^* F_i^{alarm} \neq 0 \\ 0 & \text{otherwise} \end{cases} \quad \forall i \in \Psi \tag{12}$$

where (10) and (11) can be expressed by F_i^* and F_i^{alarm} through simple arithmetic operations, as presented in (13)-(14):

$$\begin{aligned} D_{\mathrm{BFMD},i} &= \left|F_i^{alarm}\right| \left(1 - \left|F_i^*\right|\right) \\ &= \left|F_i^{alarm}\right| - \left|F_i^{alarm} F_i^*\right| \quad \forall i \in \Psi \end{aligned} \tag{13}$$

$$\begin{aligned} M_{FI,i} &= \left|F_i^*\right| \left(1 - \left|F_i^{alarm}\right|\right) \\ &= \left|F_i^*\right| - \left|F_i^* F_i^{alarm}\right| \quad \forall i \in \Psi \end{aligned} \tag{14}$$

Next, θ_i and x_i are used to express the two absolute values of F_i^* and the product term of F_i^* F_i^{alarm} as follows:

$$\begin{cases} \theta_i = \left|F_i^*\right| \\ x_i = \left|F_i^* F_i^{alarm}\right| \end{cases} \quad \forall i \in \Psi \tag{15}$$

Then the evaluation variable for distorted alarms $D_{\mathrm{BFMD},i}$ and that for missing alarms $M_{\mathrm{BFMD},i}$ can be rewritten as:

$$\begin{cases} D_{\mathrm{BFMD},i} = (F_i^{alarm})^2 - x_i \\ M_{\mathrm{BFMD},i} = \theta_i - x_i \end{cases} \quad \forall i \in \Psi \tag{16}$$

Note that in the fault diagnosis, the actual alarm F_i^{alarm} is a constant; therefore, equation (16) is linear. However, it is obvious that the expressions in (15) are not linear. To convert the formulation into a linear integer programming problem, (15) must be linearized, which is done as detailed in (17).

$$\begin{cases} -F_i^* \leq \xi_i \leq \dfrac{1 - F_i^*}{2} \\ \theta_i = F_i^* + 2\xi_i \\ x_i \leq \theta_i \\ x_i \leq (F_i^{alarm})^2 \\ x_i \geq \theta_i + (F_i^{alarm})^2 - 1 \end{cases} \quad \begin{array}{c} \forall i \in \Psi \\ x_i, \xi_i, \theta_i \in \{0, 1\} \end{array} \tag{17}$$

where θ_i, x_i and ξ_i are three binary transition variables to satisfy the relationship in (16).

Although the evaluation variable for reverse alarms $R_{\mathrm{BFMD},i}$ cannot be expressed by simple arithmetic operations, it can be set as a binary variable with equation (12) replaced by the following constraint:

$$R_{\mathrm{BFMD},i} \geq -F_i^{alarm} F_i^* \quad \forall i \in \Psi \tag{18}$$

To prove the correctness of the proposed linearization method, all possible values of the variables in (16)-(18) are shown in Table 4.

Comparing Table 3 with Table 4, it can be concluded that these three evaluation variables, along with the constraints (16)-(18), can correctly identify the states and types of false alarms.

The proposed linear integer programming model for fault diagnosis is thus completed, with an objective function (3) to be minimized subject to constraints (5)-(9), and (16)-(18).

C. THE SUITABLE FAULT TYPES

The proposed fault diagnosis model is a basic framework for alarm analysis considering communication failures, and it is suitable for all possible faults that can be detected by fault monitoring devices installed in the distribution system. To be

TABLE 4. All possible combinations of alarms and corresponding values of variables.

F_i^*	F_i^{alarm}	ξ_i	θ_i	x_i	$M_{\mathrm{BFMD},i}$	$D_{\mathrm{BFMD},i}$	$R_{\mathrm{BFMD},i}$
0	0	0	0	0	0	0	0
+1	0	0	1	0	1	0	0
0	+1	0	0	0	0	1	0
+1	+1	0	1	1	0	0	0
-1	0	1	1	0	1	0	0
0	-1	0	0	0	0	1	0
-1	-1	1	1	1	0	0	0
-1	+1	1	1	1	0	0	1
+1	-1	0	1	1	0	0	1

specific, we focus on the alarm analysis in an active distribution system rather than the technique used for detecting faults.

The types of faults that can be detected are directly related to the distribution density and detecting accuracy of the installed monitoring devices. The penetration level of the monitoring devices in different areas varies. For example, the density of the monitoring devices in a rural-area distribution system is usually lower than that in an urban distribution system. In addition, high-resistance grounding faults can only be detected by devices with high-precision sensors, which are commonly installed in the urban distribution system, but not in the rural one.

D. THE ALGORITHM AND THE FLOWCHART

The proposed model can be efficiently solved by branch and bound algorithms, which have been integrated by commercial solvers, such as CPLEX and Gurobi.

Because of the efficiency of the solution approach, the proposed fault diagnosis model can be run online by the dispatching center of the power distribution system. The solution flowchart for addressing a fault diagnosis problem is presented in Fig. 5.

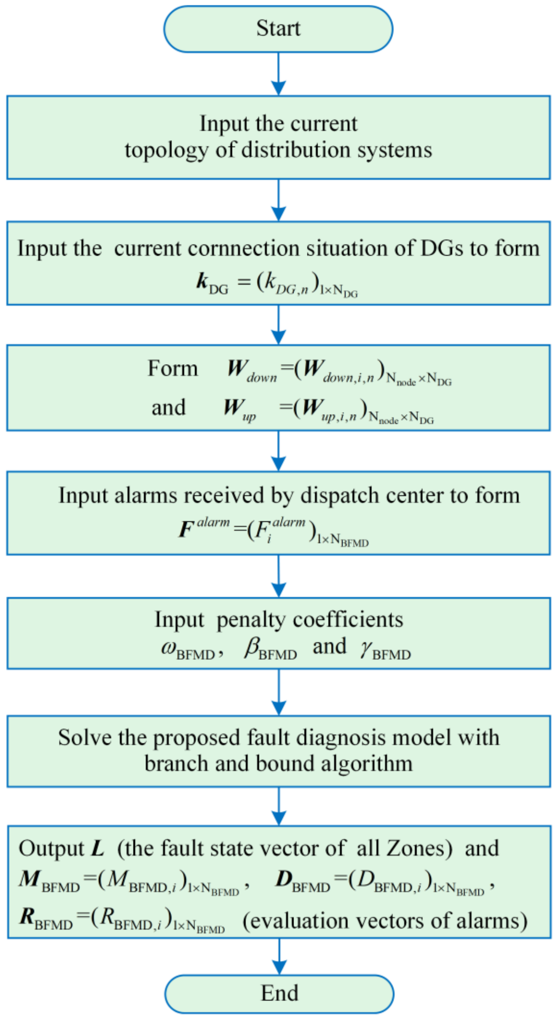

FIGURE 5. Solution flowchart for fault diagnosis.

V. CASE STUDIES

In this section the performance of the proposed method is tested in a modified IEEE 33-bus system and an actual distribution power system in Guangzhou, China. All simulations were performed on a PC with Intel Core i5 Processor (2.8 GHz) and 8-GB RAM. The proposed linear integer programming model for fault diagnosis was solved by the branch and bound algorithm integrated with the commercial optimization solver Gurobi-8.0. Yalmip/MATLAB is used as the optimization platform. Note that the calculation time in this paper was verified with the consumed CPU time that returned by Gurobi optimization solver.

The values of the three penalty coefficients involved in the objective function (3) need to be discussed.

Actually, the accuracy of fault diagnosis is affected by these three coefficients (β_{BFMD}, γ_{BFMD} and ω_{BFMD}) involved in the multi-objective function due to the diversity of the installed BFMDs in various locations. A feasible method to determine the relative magnitudes of these three coefficients by experiences of exsisting publications and seleceting the specific values of these coefficients by sensitivity tests with a standard system, such as IEEE-33 bus system.

It is also possible to examine the relationship among the values of these three coefficients based on engineering experiences. According to some exsisting papers such as refs. [24], [25], [26], and [28], generally the probability of an alarm being lost is greater than that of a distorted alarm being received. In addition, as for a false alarm sent by a bi-directional fault monitoring device, a "reverse" alarm (i.e., the sign of the alarm changes) is different from a "distorted" alarm (i.e., the content of the alarm changes). Specfically, a "reverse" alarm that indicates a fault can be received only when the sign bit changes, while a "distorted" alarm could involve more changes in relevant data. Therefore, the values of the penalty coefficients in (3) should respect the inequality: $\beta_{\mathrm{BFMD}} > \gamma_{\mathrm{BFMD}} > \omega_{\mathrm{BFMD}}$. According to sensitivity tests of the coefficients values with the IEEE 33-bus test system, the best values of β_{BFMD}, γ_{BFMD} and ω_{BFMD} can be set as 1.5, 1.3 and 1.1, respectively, whose performance analysis will be illustrated hereinafter.

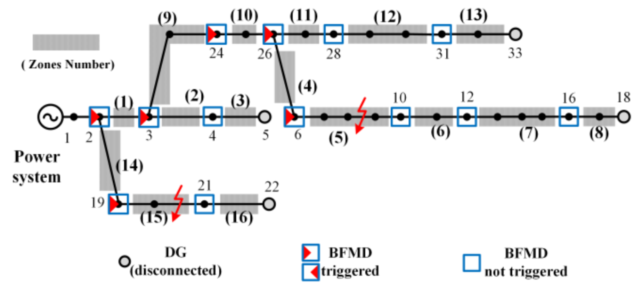

FIGURE 6. A modified IEEE 33-bus system without DG connected.

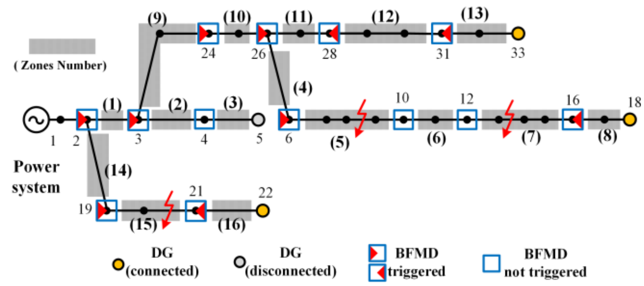

FIGURE 7. A modified IEEE 33-bus system with DGs connected.

A. FIVE CASE STUDIES WITH IEEE 33-BUS SYSTEM

1) SCENARIO I: MULTIPLE FAULTS WITH NO DG CONNECTED AND ALL ALARMS ARE CORRECT

In Fig. 6, the numbers of the nodes where BFMDs are installed have been marked. The direction indicated by the red triangle is consistent with the fault direction indicated by actual alarms received by the dispatch center. In this case, it is assumed that all alarms sent by BFMDs are correct.

As shown in Fig. 6, the feeder is separated into 16 zones with 12 BFMDs. When two three-phase grounding faults occur on zone-(5) and zone-(15), the values of actual alarms sent by BFMDs-2, 3, 6, 19, 24, and 26 can be obtained as 1, and the values of the actual alarms sent by other BFMDs are 0. After taking 0.21 seconds, the model was successfully solved, and the optimal solution is presented as follows:

$$\boldsymbol{L} = [0, 0, 0, 0, 1, 0, 0, 0, 0, 0, 0, 0, 0, 0, 1, 0];$$
$$\boldsymbol{M} = \boldsymbol{D} = \boldsymbol{R} = 0.$$

The optimal solution obtained is consistent with the scenario assumed. Specifically, the alarm of BFMD-10 indicates that the fault should not be located in its downstream (also confirmed by BFMDs-12 and 16), and the alarms of BFMDs-2, 3, 6, 24, and 26 indicate that the fault occurs downstream of node-6, so a fault-zone is determined to be zone-(5). Similarly, the alarm of BFMD-21 indicates that the fault should not be located on its downstream, and the alarms of BFMDs-2 and 19 indicate that the fault occurs downstream of node-19, so zone-(15) can be determined to be a fault zone. This analysis can be illustrated mathematically by the model proposed.

2) SCENARIO II: MULTIPLE FAULTS WITH DGs CONNECTED AND ALL ALARMS ARE CORRECT

In this scenario, three DGs are connected at nodes-18, 22 and 33, while the other part of the topology is consistent with Fig. 6. Three three-phase grounding faults are assumed to occur in zones-(5), (7) and (15), as presented in Fig. 7. Due to the different control strategies of the DG's inverter, the magnitude of the short-circuit current provided by a DG will be various. To verify whether the proposed fault diagnosis method can be effectively applied in active distribution systems with a high penetration level, the capacities of DGs-18, 22, and 33 are respectively 0.8MW, 0.8MW and 1.0MW, which are 15.7%, 15.7% and 19.7% of the total typical load power (5.084MW). Simulation results show that when a fault occurs, the minimum overcurrent produced by each DG is 2.3 times of that in the normal operating condition, and hence the fault can be easily detected by BFMDs.

Compared with scenario I, the values of alarms sent by BFMD-16, 21, 28, and 31 in scenario II are changed from 0 to −1 due to the connections of DGs. After taking 0.22 seconds, the model was solved successfully, and the optimal solution is presented as follows:

$$\boldsymbol{L} = [0, 0, 0, 0, 1, 0, 1, 0, 0, 0, 0, 0, 0, 0, 1, 0];$$
$$\boldsymbol{M} = \boldsymbol{D} = \boldsymbol{R} = 0.$$

It can be seen that the fault zones-(5), (7), and (15) can be determined accurately. Note that the alarm sent by BFMD-16 indicates that fault(s) may locate on the upstream of it and the alarm sent by BFMD-6 indicates that fault(s) may locate on the downstream direction, zones-(5), (6), and (7) are all possible fault-zones. As alarms sent by BFMD-10 and BFMD-12 indicate that there is no possibility for a fault to occur in zone-(6), both zone-(5) and zone-(7) can be determined to be the fault zones finally.

3) SCENARIO III: MULTIPLE FAULTS WITH DGs CONNECTED AND MISSING ALARMS ARE RECEIVED

Based on scenario II, to verify the performance of the fault diagnosis model when alarms are lost, the alarms sent by BFMDs-3, and 26 are set to 0 in this scenario. After 0.23 seconds of computation, the value of the optimal objective function is 5.4, and the optimal values of the variables are presented below.

$$\boldsymbol{L} = [0, 0, 0, 0, 1, 0, 1, 0, 0, 0, 0, 0, 0, 0, 1, 0];$$
$$\boldsymbol{M} = [0, 0, 1, 0, 0, 0, 0, 0, 0, 0, 0, 0, 0, 0, 0, 0, 0, 0, 0, 0, 0, 0, 0, 0, 0, 1, 0, 0, 0, 0, 0, 0, 0]; \quad \boldsymbol{D} = \boldsymbol{R} = 0.$$

It can be seen that three fault zones and the three missing alarms can be identified accurately. Note that in the evaluation vector $\boldsymbol{M}$ for missing alarms, the evaluation vector $\boldsymbol{D}$ for distorted alarms, and the evaluation vector $\boldsymbol{R}$ for reverse alarms, there are zero elements at the node indexes where no BFMDs were installed. Since there are no constraints on the variables at these nodes, their values are set to 0 because of the minimization of the objective function.

4) SCENARIO IV: MULTIPLE FAULTS WITH DGs CONNECTED AND DISTORTED ALARMS ARE RECEIVED

Based on scenario I, alarms sent by BFMD-4 and BFMD-10 are changed from 0 to −1 in this scenario, i.e., these two alarms are distorted. After taking 0.29 seconds for computation, the optimal objective value is 6.0, and the optimal values of the variables are presented below.

$$\boldsymbol{L} = [0, 0, 0, 0, 1, 0, 1, 0, 0, 0, 0, 0, 0, 0, 1, 0];$$
$$\boldsymbol{D} = [0, 0, 0, 1, 0, 0, 0, 0, 0, 1, 0, 0, 0, 0, 0, 0, 0, 0, 0, 0, 0, 0, 0, 0, 0, 0, 0, 0, 0, 0, 0, 0, 0]; \quad \boldsymbol{M} = \boldsymbol{R} = 0.$$

It can be seen that the assumed scenario IV is correctly reflected by the optimal solution. Note that as there is no DG connected to node-5, the expected alarm of BFMD-4 is constrained by the related constraints in (5)-(9).

5) SCENARIO V: MULTIPLE FAULTS WITH DGs CONNECTED AND MISSING AND REVERSE ALARMS ARE RECEIVED

Based on scenario II, assume alarms sent by BFMD-31 and BFMD-16 are changed from -1 to +1 in this scenario, i.e., the direction of fault location indicates by these two alarms are reverse. After 0.35 seconds of computation, the optimal objective value is 8.0, and the optimal values of the variables are presented below.

$$\boldsymbol{L} = [0, 0, 0, 0, 1, 0, 1, 0, 0, 0, 0, 0, 0, 0, 1, 0];$$
$$\boldsymbol{M} = [0, 0, 1, 0, 0, 0, 0, 0, 0, 0, 0, 0, 0, 0, 0, 0, 0, 0, 0, 0, 0, 0, 0, 0, 0, 0, 1, 0, 0, 0, 0, 0, 0, 0];$$
$$\boldsymbol{R} = [0, 0, 0, 0, 0, 0, 0, 0, 0, 0, 0, 0, 0, 0, 0, 1, 0, 0, 0, 0, 0, 0, 0, 0, 0, 0, 0, 0, 0, 0, 1, 0, 0]; \quad \boldsymbol{D} = 0.$$

It can be seen that three fault zones, two missing alarms and two reverse alarms are identified accurately. Although four incorrect alarms have been found by the optimal solution, there is no possibility to find a better solution. For instance, assuming that the alarm sent by BFMD-16 is determined to be correct, the only reasonable solution is that the alarms sent by BFMD-10 and BFMD-12 are lost, and zone-(8) is identified to be a fault instead of a zone-(5) and zone-(7). However, the objective value for this possible solution is 8.1, which is larger than the optimal one.

B. COMPARISON: BFMDs AND UFMDs

Most studies in literature focused on fault location methods utilizing the data collected by uni-directional fault monitoring devices, instead of the bi-directional ones. To illustrate the contribution of this paper, it is necessary to compare the performance between our proposed approach with those in literature, such as [7], [15], [26]–[28]. To facilitate the presentation, the uni-directional fault monitoring devices are abbreviated as UFMDs.

Consider the modified IEEE 33-bus system with DGs connected, as shown in Fig. 8, which is the same as Fig. 7 except that all BFMDs are replaced with UFMDs. The default directions of all UFMDs are indicated by the directions of the blue triangle in Fig. 8.

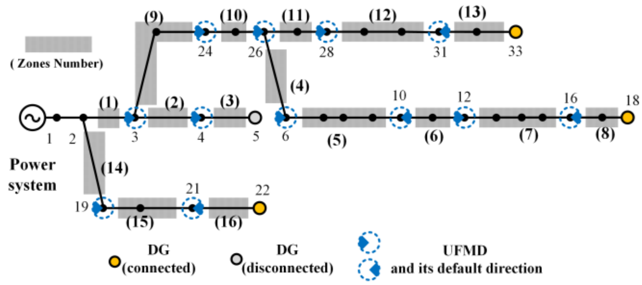

FIGURE 8. The modified IEEE 33-bus system with UFMDs.

TABLE 5. Evaluation variables of false alarms.

Scenarios	The diagnostic results with BFMDs (All Correct)		The diagnostic results with UFMDs	
	Fault zones	False alarms	Fault zones	False alarms
I	(5), (15)	M: / D: / R: /	(5), (15)	M: / D: / R: /
II	(5), (7), (15)	M: / D: / R: /	(5), (7)	M: 21, 28 D: / R: 19
III	(5), (7), (15)	M: 3, 26 D: / R: /	(7), (16)	M: 3, 21, 26 D: / R: 28
IV	(5), (7), (15)	M: / D: 4, 10 R: /	(5), (16)	M: 12, 28 D: / R: /
V	(5), (7), (15)	M: 3, 26 D: / R: 16, 31	/	M: / D: 2,6,19,24 R: /

By testing the same five scenarios with multiple faults in Section IV-A, the comparison of the results, UFMDs vs. BFMDs, is summarized in Table 5. Note that in scenario V, as the alarms sent by UFMD-16 and UFMD-31 cannot be reversed for their uni-directional monitoring function, these two alarms are set to be lost.

As can be seen from Table 5, the diagnostic results using UFMDs are correct only when there is no DG connected and the alarms sent by UFMDs are correct. With the connection of DGs (scenarios II–V), fault zone-(15) was not successfully identified, and some false alarms are identified incorrectly. As the number of false alarms increases, more fault zones found by UFMDs are missed. In scenario V, when there are insufficient false alarms and directional fault indications available, all fault zones are missed.

C. TEST WITH A 55-BUS SYSTEM IN GUANGZHOU

Next we use a 55-bus power distribution system in Guangzhou (GZ-55-bus system),as presented in Fig. 9, to test

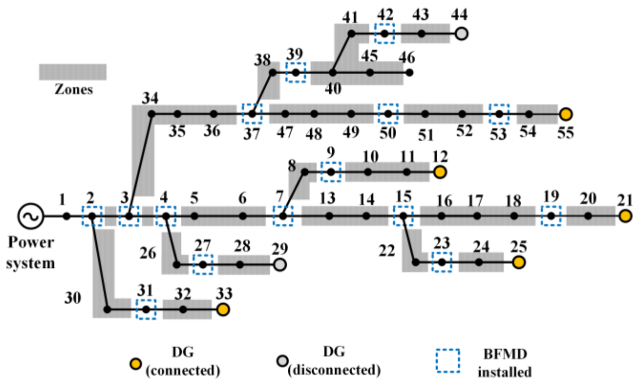

FIGURE 9. The GZ-55-bus system.

the feasibility of the online fault diagnosis by the proposed linear integer programming model.

The average CPU times and diagnostic accuracies of fault zone identification are summarized in Table 6. In each case (given the numbers of fault zones and missing alarms), 50 different fault scenarios (including missing alarms) were randomly generated and solved to calculate the average CPU time and diagnostic accuracy.

TABLE 6. Average CPU time and fault diagnosis accuracy in the GZ-55-bus system.

Number of fault zones	Number of missing alarms	Average CPU time (seconds)	Average diagnosis accuracy (identification of fault zones)
1	0	0.30	100%
	1	0.29	100%
	2	0.32	96%
	3	0.33	94%
2	0	0.38	100%
	1	0.37	88%
	2	0.36	78%
	3	0.39	70%

It can be seen that the time performance is excellent as the average CPU time is less than one second, indicating that the proposed approach can be used for the online fault diagnosis of distribution feeders for its light computational requirement. In terms of the diagnostic accuracies, when there is no missing alarm received, the results of fault diagnosis are all correct when there are one or two faults on the feeder. As can be seen from Table 6, although more missing alarms will lead to a lower accuracy rate of fault diagnosis, the number of fault zones carries more influence on the diagnosis accuracy.

D. PERFORMANCES WITH DIFFERENT SCALES OF SYSTEMS

With several tests carried out with IEEE-33 bus system and the GZ-55-bus system, the performances of the proposed fault diagnosis model different scale test systems are summarized as follows:

1) The average solving time represented by CPU time consumed in Gurobi with the IEEE 33-bus test system is 0.24 seconds for a test scenario with two simultaneous faults and two missing alarms. The average solving time with the same number of fault sections and missing alarms tested in the GZ-55-bus test system is 0.37 seconds, and meets the requirement for on-line fault diagnosis. Actually, as the fault diagnosis problem is formulated as a linear integer programming model, the increased scale of the distribution system may not necessarily lead to longer solving time since the fault diagnosis is limited to the outage area(s).

2) The increasing scale of the distribution system is not the main factor having impacts on the accuracy of the fault diagnosis results. It can be clearly seen from the numerical results in Table 6 that the number of simultaneous fault zones and the number of false alarms sent by BFMDs have significant impacts on the fault diagnosis accuracy. The fault diagnosis under scenarios with unreliable communications is an intractable issue to be investigated further.

E. COMPARISONS WITH EXISTING METHODS

Comparisons of performances between the proposed fault diagnosis method in this paper and other fault location methods proposed in recent publications are presented in Table 7.

TABLE 7. Performances comparisons between the proposed method and some available methods.

Methods	Linear or not	Factors considered				
		Missing alarms	Distorted alarms	Reverse alarms	DGs	BFMDs
[15]	×	√	√	×	√	×
[16]	√	√	√	×	×	×
[26]	×	√	√	×	×	×
[27]	√	√	×	×	√	×
[28]	√	√	√	×	√	×
This paper	√	√	√	√	√	√

F. OTHER CHALLENGES AND POSSIBLE MEASURES

The connection of distributed power sources brings great challenges to the fault identification and restoration tasks of modern power distribution systems. The types of distribution generators mainly fall into two categories: rotating electrical machine type power sources (e.g., diesel engines and gas engines) and centralized inverter interfaced renewable energy power sources (e.g., wind power or solar panel). Decentralized inverter interfaced renewable energy resources (e.g., residential PVs or small wind turbines) are not addressed in this paper. Small wind turbines and PV located on the roofs of residential customers also increase the complexity for fault monitoring devices to identify faults.

In addition to updating the thresholds that can trigger BFMDs to send an alarm in real-time according to the installation locations of specific inverters, utilizing the data collected with a high frequency by the D-PMUs and historical database to make proactive decisions is a topic for future research.

VI. CONCLUSION

A linear integer programming model for fault diagnosis in active power distribution systems is proposed in this paper. By utilizing the fault direction related alarms sent by bi-directional fault monitoring devices (such as D-PMU, FTUs, bi-directional FIs), the tasks of the estimation of fault zones and the identification of false alarms can be addressed together. In addition, by changing the input values of the corresponding variables, it is easy to adapt to the changes in the topology of the distribution system studied and the connection state of each DG. As more fault location information can be attained by the bi-directional fault monitoring devices than the uni-directional ones, the fault diagnosis method proposed can accommodate more false alarms. Simulations have demonstrated that the proposed approach is sufficiently efficient for real-time fault diagnosis of distribution systems.

ACKNOWLEDGMENT

The authors appreciate the great assistance of Prof. Chung-Li Tseng, UNSW Business School, The University of New South Wales, Sydney, Australia, for improving the quality of the presentation of this paper.

REFERENCES

[1] M. Eriksson, M. Armendariz, O. O. Vasilenko, A. Saleem, and L. Nordström, "Multiagent-based distribution automation solution for self-healing grids," *IEEE Trans. Ind. Electron.*, vol. 62, no. 4, pp. 2620–2628, Apr. 2015.

[2] S. Gill, I. Kockar, and G. W. Ault, "Dynamic optimal power flow for active distribution networks," *IEEE Trans. Power Syst.*, vol. 29, no. 1, pp. 121–131, Jan. 2014.

[3] A. Basuki, T. I. Priadi, A. P. Sari, and H. Trirohadi, "SCADA gateway, smart solution for combining conventional substation and substation automation system," in *Proc. Int. Conf. Adv. Power Syst. Autom. Protection*, Beijing, China, Oct. 2011, pp. 1268–1272.

[4] F. J. Muench and G. A. Wright, "Fault indicators: Types, strengths & applications," *IEEE Trans. Power App. Syst.*, vol. PAS-103, no. 12, pp. 3688–3693, Dec. 1984.

[5] C. Smallwood, M. Lattner, and T. Gardner, "Expansion of distribution automation with communicating faulted circuit indicators," in *Proc. Rural Electric Power Conf.*, Apr. 2011, pp. 1–6.

[6] Y. Gong and A. Guzmán, "Distribution feeder fault location using IED and FCI information," in *Proc. 64th Annu. Conf. Protective Relay Eng.*, College Station, TX, USA, Apr. 2011, pp. 168–177.

[7] J.-H. Teng, W.-H. Huang, and S.-W. Luan, "Automatic and fast faulted line-section location method for distribution systems based on fault indicators," *IEEE Trans. Power Syst.*, vol. 29, no. 4, pp. 1653–1662, Jul. 2014.

[8] Džafić, R. A. Jabr, S. Henselmeyer, and T. Đonlagić, "Fault location in distribution networks through graph marking," *IEEE Trans. Smart Grid*, vol. 9, no. 2, pp. 1345–1353, Mar. 2018.

[9] Z. Zhang, Z. Gao, S. Li, and Y. Zhao, "The method of distribution network fault location based on improved dempster-shafer theory of evidence," in *Proc. IEEE PES Asia–Pacific Power Energy Eng. Conf. (APPEEC)*, Bengaluru, India, Nov. 2017, pp. 1–5.

[10] Y. R. Rodrigues, M. Abdelaziz, and L. Wang, "D-PMU based secondary frequency control for islanded microgrids," *IEEE Trans. Smart Grid*, vol. 11, no. 1, pp. 857–872, Jan. 2020, doi: 10.1109/TSG.2019.2919123.

[11] B. Pinte, M. Quinlan, and K. Reinhard, "Low voltage micro-phasor measurement unit (μPMU)," in *Proc. IEEE Power Energy Conf. Illinois (PECI)*, Champaign, IL, USA, Feb. 2015, pp. 1–4.

[12] M. Pignati, L. Zanni, P. Romano, R. Cherkaoui, and M. Paolone, "Fault detection and faulted line identification in active distribution networks using synchrophasors-based real-time state estimation," *IEEE Trans. Power Del.*, vol. 32, no. 1, pp. 381–392, Feb. 2017.

[13] J. Ren, S. S. Venkata, and E. Sortomme, "An accurate synchrophasor based fault location method for emerging distribution systems," *IEEE Trans. Power Del.*, vol. 29, no. 1, pp. 297–298, Feb. 2014.

[14] C. Chen, J. Wang, and D. Ton, "Modernizing distribution system restoration to achieve grid resiliency against extreme weather events: An integrated solution," *Proc. IEEE*, vol. 105, no. 7, pp. 1267–1288, Jul. 2017.

[15] G. Shen, Y. Zhang, H. Qiu, C. Wang, F. Wen, M. A. Salam, L. Guo, B. Yu, and J. Chen, "Fault diagnosis with false and/or missing alarms in distribution systems with distributed generators," *Energies*, vol. 11, no. 10, pp. 2579–2590, Sep. 2018.

[16] R. He, Z. Hu, Y. Li, and T. Wang, "Fault section location method for DG-DNs based on integer linear programming," *Power Syst. Technol.*, vol. 42, no. 11, pp. 3684–3692, Nov. 2018.

[17] M.-S. Choi, S.-J. Lee, D.-S. Lee, and B.-G. Jin, "A new fault location algorithm using direct circuit analysis for distribution systems," *IEEE Trans. Power Del.*, vol. 19, no. 1, pp. 35–41, Jan. 2004.

[18] D. Carta, P. A. Pegoraro, S. Sulis, M. Pau, F. Ponci, and A. Monti, "A compressive sensing approach for fault location in distribution grid branches," in *Proc. Int. Conf. Smart Energy Syst. Technol. (SEST)*, Porto, Portugal, Sep. 2019, pp. 1–6.

[19] F. S. Wen and C. S. Chang, "Probabilistic approach for fault-section estimation in power systems based on a refined genetic algorithm," *IEE Gener., Transmiss. Distrib.*, vol. 144, no. 2, pp. 160–168, Mar. 1997.

[20] R. Dashti and J. Sadeh, "Fault section estimation in power distribution network using impedance-based fault distance calculation and frequency spectrum analysis," *IET Gener., Transmiss. Distrib.*, vol. 8, no. 8, pp. 1406–1417, Aug. 2014.

[21] R. Dashti, M. Tahavori, M. Daisy, and H. R. Shaker, "A new matching algorithm for fault section estimation in power distribution networks," in *Proc. Int. Symp. Adv. Electr. Commun. Technol. (ISAECT)*, Rabat, Morocco, Nov. 2018, pp. 1–4.

[22] B. Cai, Y. Zhao, H. Liu, and M. Xie, "A data-driven fault diagnosis methodology in three-phase inverters for PMSM drive systems," *IEEE Trans. Power Electron.*, vol. 32, no. 7, pp. 5590–5600, Jul. 2017.

[23] B. Cai, X. Shao, Y. Liu, X. Kong, H. Wang, H. Xu, and W. Ge, "Remaining useful life estimation of structure systems under the influence of multiple causes: Subsea pipelines as a case study," *IEEE Trans. Ind. Electron.*, vol. 67, no. 7, pp. 5737–5747, Jul. 2020.

[24] B. Cai, Y. Liu, and M. Xie, "A dynamic-Bayesian-network-based fault diagnosis methodology considering transient and intermittent faults," *IEEE Trans. Autom. Sci. Eng.*, vol. 14, no. 1, pp. 276–285, Jan. 2017.

[25] F. Tian, F. Wen, X. Wang, Y. Xue, and M. A. Salam, "A multi-agent system based fault diagnosis for active distribution systems," in *Proc. IEEE Innov. Smart Grid Technol. Asia (ISGT-Asia)*, Melbourne, VIC, Australia, Nov. 2016, pp. 1110–1114.

[26] W. Li, W. Chen, C. Guo, B. Zhu, and L. Xu, "Fault diagnosis method for power distribution systems based on multi-source information," in *Proc. 43rd Annu. Conf. IEEE Ind. Electron. Soc. (IECON)*, Beijing, China, Oct. 2017, pp. 244–249.

[27] K. Sun, Q. Chen, and Z. Gao, "An automatic faulted line section location method for electric power distribution systems based on multisource information," *IEEE Trans. Power Del.*, vol. 31, no. 4, pp. 1542–1551, Aug. 2016.

[28] Y. Jiang, "Toward detection of distribution system faulted line sections in real time: A mixed integer linear programming approach," *IEEE Trans. Power Del.*, vol. 34, no. 3, pp. 1039–1048, Jun. 2019.

CHONGYU WANG (Graduate Student Member, IEEE) received the B.E. degree in electrical engineering from Xi'an Jiaotong University, Xi'an, China, in 2017. He is currently pursuing the Ph.D. degree with the College of Electrical Engineering, Zhejiang University, China. His research interest includes fault diagnosis and outage management for power systems.

KAIYUAN PANG (Graduate Student Member, IEEE) received the B.E. degree in electrical engineering from Wuhan University, Wuhan, China, in 2018. He is currently pursuing the Ph.D. degree with the College of Electrical Engineering, Zhejiang University, China. His main research interests include power system restoration and smart grids.

YAN XU is with the School of Electrical and Information Engineering, Changsha University of Science and Technology, China. His research interest includes power system operation and control.

FUSHUAN WEN (Senior Member, IEEE) received the B.E. and M.E. degrees from Tianjin University, Tianjin, China, in 1985 and 1988, respectively, and the Ph.D. degree from Zhejiang University, Hangzhou, China, in 1991, all in electrical engineering.

He joined the faculty of Zhejiang University in 1991, and has been a Full Professor since 1997. He is also a part-time Distinguished Professor under the Yusheng Xue Education Foundation, Hangzhou Dianzi University, Hangzhou. He had been a University Distinguished Professor, the Deputy Dean of the School of Electrical Engineering, and the Director of the Institute of Power Economics and Electricity Markets, South China University of Technology, Guangzhou, China, from 2005 to 2009. He is a Professor with the Department of Electrical Power Engineering and Mechatronics, Tallinn University of Technology, taking leave from Zhejiang University. His research interests include power industry restructuring, power system alarm processing, fault diagnosis and restoration strategies, and smart grids and electric vehicles.

Dr. Wen is the Editor-in-Chief of *IET Energy Conversion and Economics* and a Deputy Editor-in-Chief of *Automation of Electric Power Systems*. He serves as an editor, a subject editor, and an associate editor for a few international journals.

IVO PALU (Member, IEEE) received the Ph.D. degree in electrical power engineering from the Tallinn University of Technology (TalTech), in 2009. He has taught various courses, including wind energy and electrical materials. He is currently a Professor and the Head of the Department of Electrical Power Engineering and Mechatronics, TalTech. His main research interests include wind turbine co-operation with thermal power plants and grid integration of new energy sources. He is a member of the Board of Estonian Society for Electrical Power Engineering and the Supervisory Board of Estonian Power Company Eesti Energia AS.

CHANGSEN FENG (Member, IEEE) received the B.E. degree in electrical engineering from Shandong University, Jinan, China, in 2013, and the Ph.D. degree from Zhejiang University, Hangzhou, China, in 2019. He joined the faculty of the Zhejiang University of Technology, in 2019, and is currently an Assistant Professor with the College of Information Engineering. His research interest includes optimization and control theory in power systems.